Protein Engineering, Design & Selection vol. 22 no. 8 pp. 469–478, 2009
Published online June 18, 2009 doi:10.1093/protein/gzp023

The impact of ataxin-1-like histidine insertions on polyglutamine aggregation

Murali Jayaraman, Ravindra Kodali and Ronald Wetzel[1]

Department of Structural Biology and Pittsburgh Institute for Neurodegenerative Diseases, University of Pittsburgh School of Medicine, Biomedical Sciences Tower 3, 3501 Fifth Avenue, Pittsburgh, PA 15260, USA

[1]To whom correspondence should be addressed.
E-mail: rwetzel@pitt.edu

Spinocerebellar ataxia type 1 (SCA1) is one of a group of nine expanded CAG repeat diseases, in which polyglutamine (polyQ) expansion above a threshold is associated with increased disease risk and aggregation. SCA1 is unique in which the polyQ in the disease protein, ataxin1, often contains a few His residues that appear to block toxicity. Here, we ask how His insertions affect aggregation by comparing a Q_{30} peptide with and without a centrally inserted His-Gln-His sequence. We found that at pH 7.5–8.5, His interruptions decrease polyQ aggregation rates but do not change the spontaneous growth mechanism: nucleated growth polymerization with a critical nucleus of one without non-fibrillar intermediates. The decreased aggregation rates are because of reductions in nucleation equilibrium constants. At pH 6, however, the His-interrupted peptide aggregates by a different mechanism that involves a low ThT-binding intermediate and produces a polymorphic amyloid product. In aggregates grown at pH 7.5, the His residues are solvent-accessible. Aggregates of His-inserted polyQ are good seeds for Q_{30} elongation, suggesting the potential to recruit polyQ proteins in the cell. Our data are therefore most consistent with His insertions blocking toxicity by suppressing rates and/or altering pathways of spontaneous aggregation.

Keywords: amyloid/ataxin 1/kinetics/nucleated growth polymerization/polymorphism

Introduction

Spinocerebellar ataxia type 1 (SCA1; Chung *et al*., 1993; Klement *et al*., 1998) is one of nine expanded CAG repeat diseases, neurodegenerative disorders caused by the cytotoxicity associated with long polyglutamine (polyQ) sequences harbored within specific disease proteins (Bates and Benn, 2002). For eight of the nine diseases, there is a relatively sharp transition between benign and pathological polyQ repeat lengths in the same approximate range of 35–45 Gln residues. While SCA1 is one of the diseases with a pathological repeat length cutoff in this range, it is unusual in that the predicted sequence of the SCA1 protein, ataxin-1 (AT-1), sometimes contains one to several histidine-encoding CAT codons within the CAG repeat region (Zoghbi and Orr, 1995; Klement *et al*., 1998). These CAT insertions appear to play several critical roles in controlling SCA1 risk. First, the presence of one or more CAT insertions within a CAG repeat sequence appears to greatly stabilize the trinucleotide repeat against expansions into the pathological range during replication (Klement *et al*., 1998; Bauer *et al*., 2005). In addition, however, the insertions appear to play a role at the protein level to reduce disease risk. Indirect evidence consistent with this is the observation that all expanded CAG repeats above the pathological range in patients presenting with SCA1 are devoid of CAT insertions (Zoghbi and Orr, 1995; Matsuyama *et al*., 1999). More direct evidence is that some individuals who are disease-free in spite of possessing a SCA1 allele that contains an expansion (44 codons) above the pathological threshold (approximately 40) also have four CAT codons within the CAG tract (Quan *et al*., 1995).

Disease tissues from expanded CAG repeat diseases exhibit the presence of polyQ-containing inclusions in neurons (Bates and Benn, 2002), and expansion of polyQ sequences has been demonstrated *in vitro* (Scherzinger *et al*., 1997; Chen *et al*., 2001; Klein *et al*., 2007) and *in vivo* (Krobitsch and Lindquist, 2000; Morley *et al*., 2002; Apostol *et al*., 2003) to greatly enhance the tendency of these sequences to aggregate. While there is much to be done, in each of these diseases, to characterize the nature of the aggregated species and their place in the disease mechanism, the general association of pathogenicity with aggregation propensity is well established. An attractive hypothesis for SCA1 is therefore that the effect of CAT codon interruption on expanded CAG pathology at the protein level may be owing to some kind of suppressing effect of inserted His residues on polyQ aggregation. Supporting this hypothesis, histidine residues in some other amyloid-forming proteins are thought to play important roles in controlling aggregation (Fraser *et al*., 1994; Abedini and Raleigh, 2005). In a preliminary SCA1-related study, Sharma *et al*. found that the solubility of a model Q_{22} peptide was improved when interrupted with His residues (Sharma *et al*., 1999). This group went on to show that four His residues added within the polyQ tract, in an identical pattern to that found to block disease in a SCA1 allele (Frontali *et al*., 1999), do not alter the random coil circular dichroism spectra of monomeric polyQ in native, aqueous buffer, but do qualitatively retard the aggregation kinetics of the peptides into β-sheet-rich aggregates (Sen *et al*., 2003). A structural model was proposed in which the His residues are placed in reverse turns in the β-sheet network of the resulting aggregates (Sen *et al*., 2003). However, no data supporting this model were provided.

Previously, our group characterized in detail the aggregation of the simple polyGln sequences that are the only obvious ubiquitous feature of the nine expanded CAG repeat disease proteins (Chen *et al*., 2001; Chen *et al*., 2002a, b; Bhattacharyya *et al*., 2005; Slepko *et al*., 2006). We found that the aggregation rate increases as repeat length increases, consistent with a role for polyQ aggregation in controlling disease risk and severity (Chen *et al*., 2001). We found that the spontaneous aggregation of simple polyQ sequences occurs via a nucleated growth polymerization mechanism with a critical nucleus of one (Chen *et al*., 2002b). We also developed a method to determine the second-order

elongation rate constant for aggregation and thereby extract the nucleation equilibrium constant, which proves—as expected—to be a very low number (Bhattacharyya *et al*., 2005) confirming the expected thermodynamic instability of the nucleus (Ferrone, 1999). More recently we found that sequences flanking the polyQ sequence in the disease protein can have profound effects on the rate of aggregation, the stability/solubility of the aggregates formed, and even the aggregation mechanism (Bhattacharyya *et al*., 2006; Thakur *et al*., 2009).

In this paper we apply these methods to a study of the effects of inserted His residues within a polyQ sequence on various aspects of aggregation. We find that His insertion generally diminishes aggregation kinetics by different mechanisms depending on pH. These effects appear to be realized primarily through modulation of the thermodynamics of nucleus formation, and hence have implications for the nature of the critical nucleus. We also find that His insertion decreases the stability of the final aggregates. We also provide data on aggregate structure, some of which supports a previous structural model placing the His residues in solvent-exposed reverse turns within the aggregate. These results, along with previous studies, suggest constraints on the molecular mechanism for how insertions of two to four CAT codons in expanded CAG repeat sequences might temper toxicity operating at the protein level.

Materials and methods

Materials

PolyQ peptides such as $K_2Q_{30}K_2$, $K_2Q_{15}HQHQ_{15}K_2$ and PEG-Biotin-labeled $K_2Q_{30}K_2$ (Osmand *et al*., 2006) were synthesized at the Keck Biotechnology Center, Yale University. Peptides were designed to contain flanking pairs of Lys residues to improve handling ability. PolyQ peptides were purified and subjected to a disaggregating protocol (O'Nuallain *et al*., 2006).

Aggregation kinetics

For the spontaneous aggregation kinetics of polyQ, reactions were initiated using disaggregated peptides. All aggregation reactions were carried out at various pH values of phosphate-buffered saline containing 0.05% sodium azide ('PBSA'). The aggregation reaction was monitored through determining the concentration of monomeric polyQ remaining in solution at each time point using reverse-phase high-performance liquid chromatography (HPLC) on centrifugation supernatants, and subjecting reaction mixture aliquots to Thioflavin T fluorescence measurements (O'Nuallain *et al*., 2006). For seeded aggregation reactions, 5% of preformed aggregates (w/w) were used. Biotin-labeled $K_2Q_{30}K_2$ was incubated with aliquots of the aggregate stock suspensions used for seeding kinetics to determine the number of growing ends. Nucleation kinetics analysis was carried out to determine the critical nucleus (n^*), the nucleation equilibrium constant (K_{n^*}), and the second-order elongation rate constant (k_+) using the equation $\Delta = \frac{1}{2}K_{n^*}\ k_+^2 C^{n^*+2} t^2$ as described previously (Bhattacharyya *et al*., 2005; O'Nuallain *et al*., 2006). Briefly, a log–log plot of the initial aggregation kinetics versus concentration yields a slope from which can be calculated the critical nucleus ($n^* = \text{slope} - 2$) and a complex parameter composed of both K_{n^*} and k_+. Independent determination of the pseudo-first-order elongation rate constant k^*, and the molar concentration of viable growth points in the seed fibrils, allows calculation of the second-order elongation rate constant, k_+. This value can then be used to calculate K_{n^*}.

Covalent modification of histidine imide group at the fibrillar level

Monomeric peptide and aggregates were treated with the alkylating agent iodoacetate to modify the side chain imide group of histidine. Samples with a peptide concentration of 1 mg/ml were incubated over a period of time in argon-purged 10 mM PBSA buffer at 37°C with 10 mM iodoacetate for 3 days at pH 6.0 (Crestfield *et al*., 1963; Shivaprasad and Wetzel, 2006). Aggregate reaction mixtures were centrifuged and the pellets dissolved in 20% formic acid, and immediately analyzed by HPLC-mass spectrometry. Monomer reaction time points were directly dissolved in 20% formic acid and similarly analyzed. Using Agilent software, the mass distribution data at various HPLC elution times were deconvoluted to allow extraction of relative abundances of unmodified, singly-modified, and doubly-modified peptides. These relative abundances were used to calculate percent modification.

FTIR spectroscopy

An MB series spectrophotometer with PROTA software (ABB Bomem) was used for Fourier transform infrared spectrum of polyQ fibrils at room temperature. Samples were prepared by centrifuging at 14 000 rpm and re-suspending in PBSA. Spectra of 400 scans were recorded at 4 cm^{-1} resolution. The fibril spectra were corrected for buffer and the area of the amide I region (1600–1700 cm^{-1}) was normalized to one for the primary spectra by using PROTA software. The second derivative spectra for the amide I region were calculated from the primary spectra using the PROTA software. FTIR secondary structure assignments are from reference (Jackson and Mantsch, 1995).

Electron microscopy

A 3 μl suspension of polyQ fibrils were placed on a freshly glow-charged carbon-coated 400 mesh size copper grid and allowed to adsorb for 2 min, then washed with deionized water. The grids were then negatively stained with 2 μl of 1% uranyl acetate visualized under Tecnai T12 microscope with a magnification of ×30 000. The TEM images were captured with an UltraScan 1000 CCD camera (Gatan, Pleasanton, CA, USA) with post-column magnification of ×1.4.

Data analysis

Aggregation kinetics data were fitted in Sigma plot (version 10) to either three- or four-parameter equations (exponential decay, exponential rise to maximum or sigmoidal) or linear. Reported R^2 values and standard deviation are from the Sigma plot-fits.

Results

The *SCA1* gene encodes polyQ repeats typically interrupted by one to two His residues (Chung *et al*., 1993; Orr *et al*.,

1993). We therefore investigated the effect of His-interruption on polyQ aggregation, using a model peptide sequence $K_2Q_{15}HQHQ_{15}K_2$, with a $K_2Q_{30}K_2$ peptide used as control. As in all of our studies of simple polyQ aggregation, the polyQ sequence is flanked by pairs of lysine residues in order to confer kinetic solubility onto the peptides, so that their aggregation kinetics can be studied from a soluble monomeric state (Chen *et al*., 2001; Chen *et al*., 2002a, b; O'Nuallain *et al*., 2006; Wetzel, 2009).

Basic trends in aggregation kinetics

We assessed the aggregation of both peptides in PBSA solutions at different pH values at 37°C by monitoring the time-dependence of both the loss of monomer from solution (Fig. 1A) and the development of a ThT signal (Fig. 1B) (O'Nuallain *et al*., 2006). Both measures show that $K_2Q_{15}HQHQ_{15}K_2$ aggregates more slowly than $K_2Q_{30}K_2$ at all pH values investigated. Thus, at pH 7.5, a 37 μM solution of $K_2Q_{30}K_2$ (open triangles) is about 75% aggregated after 4 days, while an identical concentration of $K_2Q_{15}HQHQ_{15}K_2$ (filled triangles) aggregates only about 10% to completion over the same period (Fig. 1A and B). For both $K_2Q_{30}K_2$ (open symbols) and $K_2Q_{15}HQHQ_{15}K_2$ (closed symbols), aggregation rate systematically drops as pH decreases from 8.5 (open circles, closed circles) to 6.0 (open squares, filled squares). Neither peptide aggregates appreciably at pH 5.5 (data not shown).

Importantly, the rates of progression of the aggregation reactions at pH 7.5 and 8.5 are remarkably similar, whether monitored by ThT or by the sedimentation assay. Thus, a plot of reaction progress as measured by ThT versus reaction progress measured by sedimentation, for reactions for both peptides at pH 7.5 and 8.5, yields a straight line with no data points significantly off the line (Fig. 1C). This parallel development of the two signals, even at early time points (Fig. 1C inset), is an indication of no significant non-fibrillar

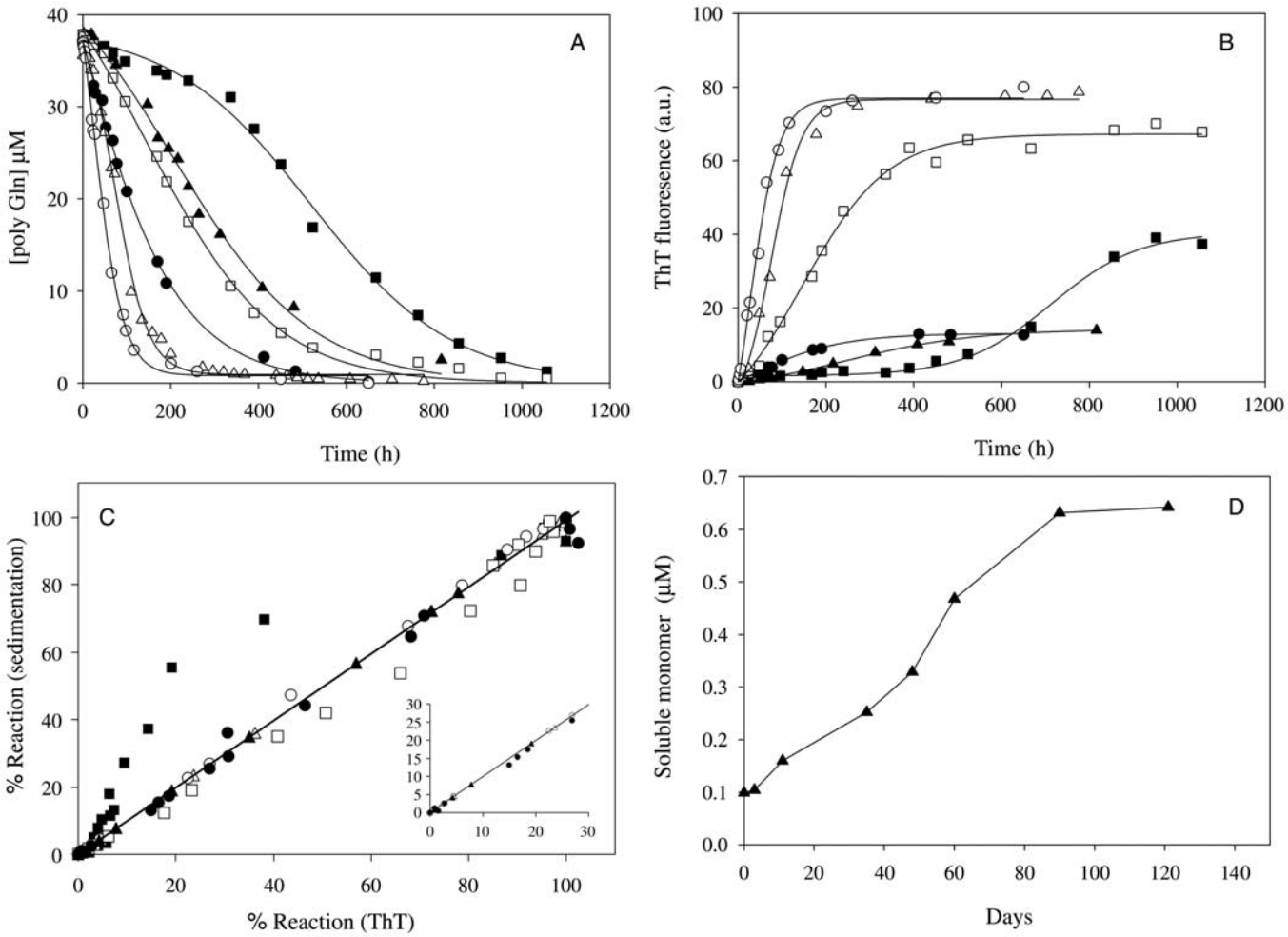

Fig. 1. Aggregation kinetics of polyQ peptides. Spontaneous aggregation of polyQ peptides incubated at approximately 37 μM in PBSA at 37°C. (**A**) Monitored by the decrease in the concentration of soluble peptide of $K_2Q_{30}K_2$ at pH 6.0 (open squares, $R^2 = 0.9975$, SD = ±0.80), pH 7.5 (open triangles, $R^2 = 0.9968$, SD = ±0.82) and pH 8.5 (open circles, $R^2 = 0.9984$, SD = ±0.66), and of $K_2Q_{15}HQHQ_{15}K_2$ at pH 6.0 (filled squares, $R^2 = 0.9960$, SD = ±0.90), pH 7.5 (filled triangles, $R^2 = 0.9949$, SD = ±0.86) and pH 8.5 (filled circles, $R^2 = 0.9984$, SD = ±0.57). (**B**) Monitored by increase in ThT signal for $K_2Q_{30}K_2$ at pH 6.0 (open squares, $R^2 = 0.9898$, SD = ±3.03), pH 7.5 (open triangles, $R^2 = 0.9936$, SD = ±3.04) and pH 8.5 (open circles, $R^2 = 0.9965$, SD = ±2.20), and for $K_2Q_{15}HQHQ_{15}K_2$ at pH 6.0 (filled squares, $R^2 = 0.9930$, SD = ±1.23), pH 7.5 (filled triangles, $R^2 = 0.9980$, SD = ±0.28) and pH 8.5 (filled circles, $R^2 = 0.9961$, SD = ±0.33). (**C**) Plot of extent of reaction monitored by sedimentation assay (A) versus extent of reaction as monitored by ThT (B) for the six combinations of peptide and pH shown in parts (A) and (B). (**D**) Dissociation kinetics of the pH 7.5 $K_2Q_{15}HQHQ_{15}K_2$ aggregate incubated in PBSA at 37°C, as monitored by the high-performance liquid chromatography sedimentation assay. At the start of incubation, the aggregate suspension contained an equivalent of about 1.5 μM $K_2Q_{15}HQHQ_{15}K_2$. The plateau of monomer concentration (C_r) is 0.63 ± 0.07 μM.

intermediates in the nucleated growth pathway, a feature noted previously for the spontaneous nucleation of various polyQ peptides at pH 7.5 (Chen *et al.*, 2002a, b). In contrast, there is a dramatic non-linearity in Fig. 1C for $K_2Q_{15}HQHQ_{15}K_2$ at pH 6 (filled squares). In this reaction, development of the ThT signal significantly lags behind that of the sedimentation assay, suggesting the presence of an intermediate with a relatively poor response to ThT. We reported a similar result recently for polyQ sequences that include the 17 amino acid huntingtin N-terminus (Thakur *et al.*, 2009). Consistent with a less ThT-sensitive intermediate, EM grids from early time points of the pH 6.0 reaction of the His peptide exhibit a mixture of fibrillar and spherical oligomeric structures (not shown). The Q_{30} peptide also exhibits some irregularity in its aggregation at pH 6.0, with reaction extent measured by ThT in this case developing somewhat more rapidly than measured by sedimentation (Fig. 1C; □). The significance and basis of this relatively small effect, only observed at pH 6.0, is not clear.

The ThT data (Fig. 1B) also suggest some structural differences among these aggregates. Since all six of these reactions were initiated with essentially the same concentration of peptide, and since they all proceeded essentially to completion, we can be sure that the ThT signal measured at the end of the reactions reflect essentially the same mass of aggregates. It is clear, therefore, that while the aggregates formed by Q_{30} at pH 7.5 and 8.5 are identical, with respect to ThT fluorescence yield, the pH 6.0 Q_{30} aggregate may have an altered structure with a somewhat lower ThT response. More dramatically, while $K_2Q_{15}HQHQ_{15}K_2$ gives apparently identical aggregates grown at pH 7.5 and 8.5, the aggregates grown at pH 6.0 are substantially different, yielding a much higher ThT response. In general, the Q_{30} aggregates give much higher ThT responses than $K_2Q_{15}HQHQ_{15}K_2$ aggregates, but whether this is because of different aggregate folded structures, or the presence of surface His residues that might influence ThT binding, cannot be determined. Point mutations in amyloidogenic peptides can have dramatic differences on the ThT fluorescence yields of their aggregates (Shivaprasad and Wetzel, 2006). In addition, however, polymorphic forms of the same peptide sequence can also exhibit strong ThT differences (R. Kodali and R. Wetzel, manuscript submitted).

Critical concentration for fibril assembly

$K_2Q_{15}HQHQ_{15}K_2$ incubated at pH 7.5 at 37°C exhibits an easily measured amount of monomer in solution (approximately 2.5 μM) even after 800 h reaction time (Fig. 1A). The $K_2Q_{30}K_2$ peptide, in contrast, has about 0.2 μM of monomer remaining. To probe the explanation of the 2.5 μM monomer levels, we diluted a sample of this reaction mixture to a total peptide concentration (i.e. monomer plus aggregates) in PBSA of 1–2 μM and incubated at 37°C. We observed a very slow off-rate of $K_2Q_{15}HQHQ_{15}K_2$ monomer over a 100-day period to a plateau of 0.63 μM (Fig. 1D). This value for C_r, the monomer concentration in equilibrium with aggregates, is the reciprocal of the equilibrium constant for fibril elongation (O'Nuallain *et al.*, 2005) which, by calculation, is thus 1.59×10^6 M. Because of its low value, we were not able to accurately determine a C_r for $K_2Q_{30}K_2$ under these conditions, but clearly it can be no greater than 0.2 μM. Fibrils of $K_2Q_{15}HQHQ_{15}K_2$ are thus at least three to four times less stable against dissociation than $K_2Q_{30}K_2$ fibrils.

Nucleation kinetics analysis

To probe the basis of the different aggregation kinetics seen at pH 7.5 and 8.5 in Fig. 1, we studied the nucleation kinetics for aggregation of these two peptides. Although spontaneous amyloid growth reactions are often said to exhibit a lag phase, true extended baseline lag phases are normally only observed when nucleation is exaggerated by secondary nucleation effects (Ferrone, 1999). While such secondary nucleation events generate dramatic and clear lag phases, they can also complicate kinetic analysis of the nucleation mechanism (Collins *et al.*, 2004) by obscuring the primary nucleation event. For reasons that are structurally unclear, polyQ fibrils are consistently resistant to such secondary nucleation phenomena. This fortuitous property allows analysis of the early aggregation kinetics to probe the basis of the more obscure primary nucleation event (O'Nuallain *et al.*, 2006).

Using the sedimentation assay, we determined the concentration dependence of aggregation at pH 7.5 and 8.5 for rigorously disaggregated samples of Q_{30} peptides with and without the inserted His-Gln-His (Fig. 2). The initial time points were analyzed by a plot of peptide concentration versus time^2 (Supplementary data are available at *PEDS* online, Figure S1). The rates were plotted versus starting concentration on a log–log plot (Fig. 3A). These data gave very good linear fits with slopes in the range of 2.5–3, as found for the analysis of other polyQ peptides (Chen *et al.*, 2002b; Thakur and Wetzel, 2002; Bhattacharyya *et al.*, 2005; Bhattacharyya *et al.*, 2006; Slepko *et al.*, 2006; Wetzel, 2009). These slopes correspond to a critical nucleus of approximately 1 for each peptide and pH analyzed. Pseudo-first-order elongation rate constants (k^*) were determined for the self-seeded elongation of both peptides at both pH 7.5 and 8.5 (Fig. 3B), the molar concentrations of the growing ends of the seeds employed were titrated using biotinyl-Q_{30} (Bhattacharyya *et al.*, 2005) (Fig. 3C), and the values combined to calculate the k_+ values (Table I). These values were used to determine K_{n^*} (Table I). As suggested for the visually parallel lines in Fig. 3A and confirmed by the values in Table I, there appear to be no fundamental differences in mechanism for peptides with or without a His insertion in the pH 7.5–8.5 range.

Using the above approach, we previously reported a K_{n^*} value of 2.6×10^{-9} for $K_2Q_{47}K_2$, corresponding to a free energy of 12.2 kcal/mol (using the expression of $\Delta G = -RT \ln K_{eq}$) for the pre-equilibrium between the ground state monomer and the monomeric nucleus. As expected (Chen *et al.*, 2002b), the values for K_{n^*} determined here for $K_2Q_{30}K_2$ are lower than for $K_2Q_{47}K_2$, in the range of 10^{-11} at both pH 7.5 and 8.5. In contrast, the k_+ values for $K_2Q_{30}K_2$ at the two pH values are in the same range (approximately $10^4\ M^{-1}s^{-1}$) as that for $K_2Q_{47}K_2$ (Table I). Thus, although in general the efficiency of nucleation depends on k_+ as well as K_{n^*} (Slepko *et al.*, 2006), the slower spontaneous aggregation for $K_2Q_{30}K_2$, compared with $K_2Q_{47}K_2$, is due mostly to the more efficient K_{n^*}.

Similarly, the values in Table I reveal details of the underlying parameters on how pH changes and His insertions influence aggregation. For example, the effect on the K_{n^*}

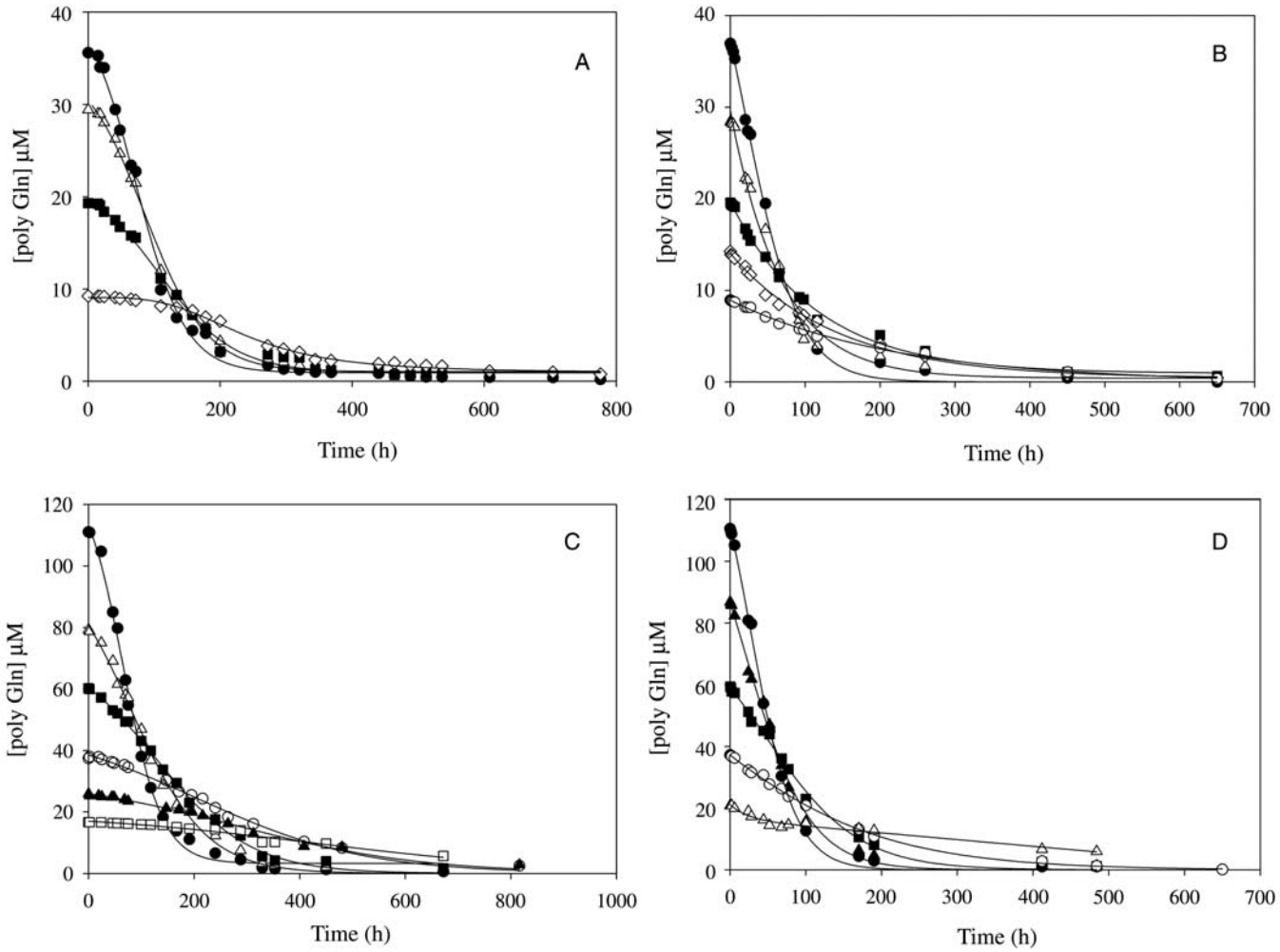

Fig. 2. Concentration-dependent aggregation in PBSA at 37°C of $K_2Q_{30}K_2$ and $K_2Q_{15}HQHQ_{15}K_2$ at pH 7.5 and 8.5 for nucleation kinetics analysis. (**A**) $K_2Q_{30}K_2$, pH 7.5 (filled circles, 35.58 μM, $R^2 = 0.9965$, SD = ±0.86; open triangles, 29.42 μM, $R^2 = 0.9930$, SD = ±0.95; filled squares, 19.29 μM, $R^2 = 0.9956$, SD = ±0.53; open diamonds, 9.23 μM, $R^2 = 0.9964$, SD = ±0.21); (**B**) $K_2Q_{30}K_2$, pH 8.5 (filled circles, 36.96 μM, $R^2 = 0.9977$, SD = ±0.76; open triangles, 28.44 μM, $R^2 = 0.9930$, SD = ±1.01; filled squares, 19.57 μM, $R^2 = 0.9964$, SD = ±0.44; open diamonds, 14.26 μM, $R^2 = 0.9964$, SD = ±0.30; open circles, 8.94 μM, $R^2 = 0.9965$, SD = ±0.18); (**C**) $K_2Q_{15}HQHQ_{15}K_2$, pH 7.5 (filled circles, 111.02 μM, $R^2 = 0.9945$, SD = ±2.73; open triangles, 79.25 μM, $R^2 = 0.9760$, SD = ±1.96; filled squares 60.22 μM, $R^2 = 0.9974$, SD = ±1.15; open circles, 37.45 μM, $R^2 = 0.9949$, SD = ±0.86; filled triangles, 25.9 μM, $R^2 = 0.9898$, SD = ±0.74; open squares, 16.67 μM, $R^2 = 0.9543$, SD = ±0.72); (**D**) $K_2Q_{15}HQHQ_{15}K_2$, pH 8.5 (filled circles, 110.57 μM, $R^2 = 0.9986$, SD = ±1.76; filled triangles, 86.84 μM, $R^2 = 0.9964$, SD = ±2.16; filled squares, 59.45 μM, $R^2 = 0.9961$, SD = ±1.44; open circles, 37.2 μM, $R^2 = 0.9984$, SD = ±0.57; open triangles, 20.83 μM, $R^2 = 0.975$, SD = ±0.83). (For time^2 plots of the initial time points, see Supplementary data are available at *PEDS* online.)

value appears to determine the reduced spontaneous aggregation rate in polyQ-containing His residues. Thus, the effect of His insertion on second-order elongation rate constant is modest, with ratios of the k_+ values for $K_2Q_{30}K_2$ to $K_2Q_{15}HQHQ_{15}K_2$ of 1.4 at pH 7.5 and 1.2 at pH 8.5. In contrast, the K_{n^*} value for $K_2Q_{30}K_2$ is approximately 21-fold higher than that for $K_2Q_{15}HQHQ_{15}K_2$ at pH 7.5, and approximately 28-fold higher at pH 8.5. The effect of these apparently conservative mutations on the ability of a polyQ peptide to form a nucleus may hold important clues into the nature of nucleus formation and structure (see Discussion).

How the nucleation kinetics parameters underlie changes in the rates of spontaneous aggregation for each peptide when comparing pH 7.5–8.5 are illustrative of the subtle interplay between K_{n^*} and k_+ in determining overall nucleation efficiency. Elongation rate constant plays an important role in nucleation efficiency, since it helps determine the percentage of nuclei that go forward to develop into a growing fibril (Slepko *et al*., 2006). An increase in elongation rate, due either to an increase in the rate constant, or an increase in the concentration of total polyQ, can improve nucleation efficiency without changing K_{n^*} (Slepko *et al*., 2006). Both $K_2Q_{30}K_2$ and $K_2Q_{15}HQHQ_{15}K_2$ aggregate more rapidly at pH 8.5 than at 7.5. The $K_2Q_{30}K_2$ peptide achieves this through more favorable values for both K_{n^*} and k_+ (Table I). In contrast, $K_2Q_{15}HQHQ_{15}K_2$ achieves this purely by an increase in k_+, since the K_{n^*} value for pH 8.5 is actually slightly less favorable than the pH 7.5 value (Table I).

Aggregate structures and properties

The reduced aggregation kinetics observed for the $K_2Q_{15}HQHQ_{15}K_2$ may be responsible for the apparently decreased toxicity of His-interrupted, expanded polyQ sequences (Quan *et al*., 1995). However, there may also be a

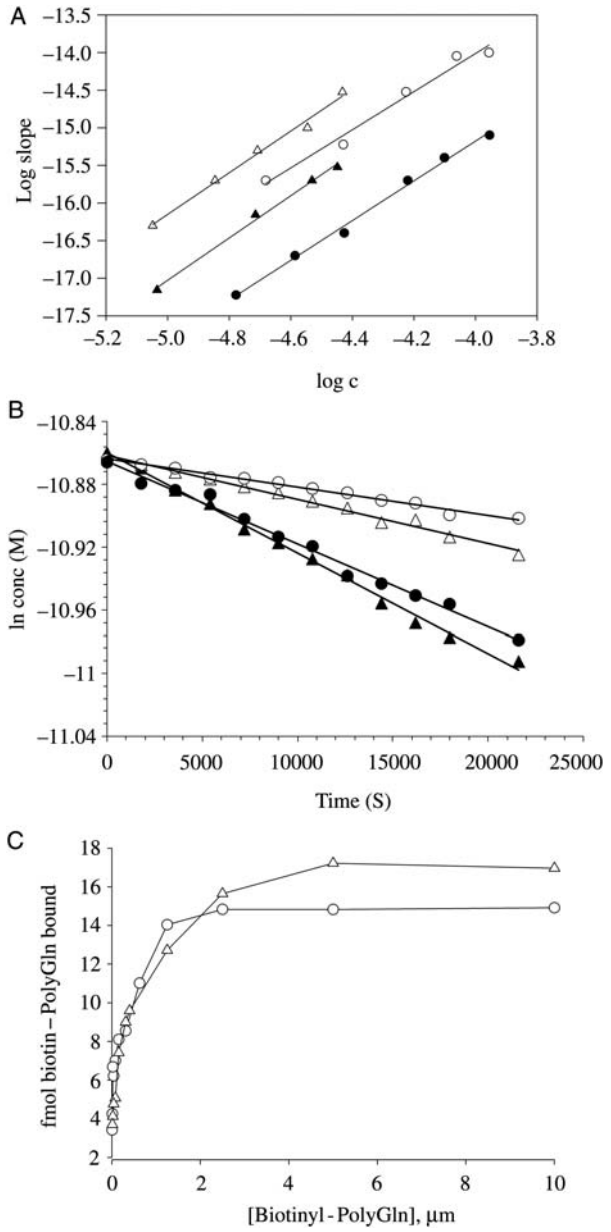

Fig. 3. Nucleation kinetics analysis for peptides at pH 7.5 and 8.5. (A) Log–log plots of initial reaction rates (from time^2 plots; see Supplementary data are available at *PEDS* online) versus initial concentration for $K_2Q_{15}HQHQ_{15}K_2$ at pH 7.5 (filled circles, slope = 2.64, $R^2 = 0.9950$, SD = ±0.06) and pH 8.5 (open circles, slope= 2.54, $R^2 = 0.9799$, SD = ±0.12), and for $K_2Q_{30}K_2$ aggregation at pH 7.5 (filled triangles, slope= 2.81, $R^2 = 0.9951$, SD = ±0.06), and pH 8.5 (open triangles, slope= 2.77, $R^2 = 0.9907$, SD = ±0.07). (**B**) Determination of pseudo-first-order elongation rate constants (k^*) from elongation kinetics of 20 μM monomers seeded with 5% (w/w) aggregates. $K_2Q_{30}K_2$, pH 7.5 (open triangles), $R^2 = 0.9885$, $k^* = 3 \times 10^{-6}\ s^{-1}$; $K_2Q_{15}HQHQ_{15}K_2$, pH 7.5 (open circles), $R^2 = 0.9867$, $k^* = 2 \times 10^{-6}\ s^{-1}$; $K_2Q_{30}K_2$, pH 8.5 (filled triangles), $R^2 = 0.9953$, $k^* = 6 \times 10^{-6}\ s^{-1}$; $K_2Q_{15}HQHQ_{15}K_2$), pH 8.5 (filled circles), $R^2 = 0.9895$, $k^* = 5 \times 10^{-6}\ s^{-1}$. (**C**) Titration of growth site concentrations in seed fibril suspensions used in part (B), using biotinylated polyQ as described (Bhattacharyya *et al*., 2005). Different concentrations of biotinyl-polyQ were incubated in 200 ng/ml aggregate at 25°C for 30 min and the aggregates washed by centrifugation then exposed to europium–streptavidin, washed and the europium fluorescence determined (Bhattacharyya *et al*., 2005; O'Nuallain *et al*., 2006). Growing end concentrations for these 200 ng/ml suspensions were determined to be 3.72×10^{-10} M for $K_2Q_{30}K_2$ aggregates (open triangles) and 3.6×10^{-10} M for $K_2Q_{15}HQHQ_{15}K_2$ aggregates (open circles). Values were used to calculate second-order elongation rate constants from the above k^* values (Table I).

role for aggregate structure. We compared the structures and properties of various $K_2Q_{30}K_2$ and $K_2Q_{15}HQHQ_{15}K_2$ aggregates by a number of methods.

The secondary structures of these aggregates were analyzed by FTIR spectroscopy. We found that aggregates of $K_2Q_{30}K_2$ and $K_2Q_{15}HQHQ_{15}K_2$ exhibited very similar, quite simple FTIR spectra (Fig. 4A), giving major bands at wavelengths 1606.5 cm^{-1} (Gln side chain NH_2 deformations), 1625.8 cm^{-1} (β-sheet) and 1656.7 cm^{-1} (Gln side chain C = O stretch).

It is particularly important to understand how the polyQ aggregate structure accommodates His side chains. Since His has only a few more atoms than Gln, is equally capable of H-bonding, and at neutral pH, is—like Gln—uncharged, it is possible that His might be readily incorporated into the polyQ β-sheet core. To test this, we addressed the accessibility of the His side chains to alkylation by iodoacetate. Previously we used alkylation of Cys residues to determine solvent accessibility of different residue positions in Aβ amyloid fibrils (Shivaprasad and Wetzel, 2006). Here, we isolated $K_2Q_{15}HQHQ_{15}K_2$ aggregates, resuspended them in buffer, and challenged them with 10 mM iodoacetate. Aggregates were periodically isolated and analyzed by LC-MS. The results (Fig. 4B) show that both His residues are solvent-accessible, but are modified at different rates. One His residue per peptide is modified within 10 h of incubation, with the remaining His residue requiring an additional 30 h of incubation to be modified. (Under similar conditions, complete modification of the His residues in the monomer occurs after about 1 h; data not shown.) It is not clear whether this kinetic discrimination between the two His residues is because they are intrinsically in different environments in the aggregate, or modification of one His alters the reactivity of the other His (Crestfield *et al*., 1963). In any case, it seems very likely that both are located in solvent-exposed structure within the fibril. While, in principle, it is possible that some alkylation within the aggregate might occur by monomer dissociation, modification and reassociation, we think this can account, at best, for very little incorporation of carboxymethyl groups, because it would be limited by the very slow monomer dissociation rate of these aggregates (Fig. 1D).

We also obtained negative stain electron micrographs for the final fibrils of each of the six aggregation reactions described here. We found that $K_2Q_{30}K_2$ aggregates produced in PBSA at pH 6–8.5 at 37°C (Fig. 5D–F) are ribbon/plate-like structures very similar to those we described previously for $K_2Q_{20}K_2$ and $K_2Q_{37}K_2$ aggregates grown in pH 7.5 PBSA (Chen *et al*., 2002a). Although all aggregates of $K_2Q_{15}HQHQ_{15}K_2$ are also basically filamentous, when formed at different pH values they each have their own individual attributes. Aggregates of $K_2Q_{15}HQHQ_{15}K_2$ grown at pH 7.5 exhibit two forms, one consisting of small plates, and the other, large bundles of long, single filaments (Fig. 5B). Both are morphologies previously seen for other polyQ aggregates (Chen *et al*., 2002a; Thakur and Wetzel, 2002). Aggregates of $K_2Q_{15}HQHQ_{15}K_2$ grown at pH 8.5 are exclusively short rods and small, fragmented plates (Fig. 5C). Aggregates of $K_2Q_{15}HQHQ_{15}K_2$ grown at pH 6.0 exhibit a very strong and different fibrillar morphology. These straight, rather thick fibrils are not normally seen in aggregates of simple polyQ peptides, but we recently reported very similar

Table I. Thermodynamic and kinetic parameters of polyQ aggregation

Peptide	fmol biotin-Q_{30}	fmol/μg aggregate	[Growing end], M	k_+ (M^{-1}, s^{-1})	Log–log Y-axis intercept	K_{n^*}	ΔG_{n^*} (kcal/mol)	n^*
$K_2Q_{47}K_2$ (pH 7.5)[a]	21.1	221	4.2×10^{-10}	1.14×10^4	−0.76	2.6×10^{-9}	12.2	0.87
$K_2Q_{30}K_2$ (pH 7.5)	17	85	3.72×10^{-10}	0.81×10^4	−2.985	3.18×10^{-11}	14.31	0.81
$K_2Q_{15}HQHQ_{15}K_2$ (pH 7.5)	15	75	3.6×10^{-10}	0.56×10^4	−4.869	8.61×10^{-13}	16.45	0.57
$K_2Q_{30}K_2$ (pH 8.5)	17	85	3.72×10^{-10}	1.61×10^4	−2.3047	3.82×10^{-11}	14.20	0.77
$K_2Q_{15}HQHQ_{15}K_2$ (pH 8.5)	15	75	3.6×10^{-10}	1.39×10^4	−3.93	1.20×10^{-12}	16.25	0.56

[a]From Bhattacharyya *et al*. (2005). See this reference as well for detailed explanation of the parameters listed in this table.

morphologies for aggregates of huntingtin (htt) exon1 peptides composed of polyQ flanked by a 17 amino acid N-terminal sequence (that contains no histidine residues) (Thakur *et al*., 2009). While the basis of this morphological similarity is not clear, it is interesting that both htt exon1 peptides aggregated at pH 7.5, and $K_2Q_{15}HQHQ_{15}K_2$ aggregated at pH 6.0, are unusual in exhibiting a low ThT-binding intermediate prior to fibril nucleation.

The above evidence for some effects of His insertions on aggregation structure is consistent with the possibility that reduced toxicity may derive, not from reduced aggregation rates, but because of some critical change in aggregate properties. Although much remains to be learnt about how various aggregated states disrupt cellular function, one attractive mechanism for polyQ toxicity is the recruitment–sequestration mechanism (Huang *et al*., 1998; Perez *et al*., 1998; Preisinger *et al*., 1999; McCampbell *et al*., 2000; Chen *et al*., 2001; Nucifora *et al*., 2001) according to which recruitment by polyQ aggregates reduces the levels of important polyQ-containing cellular factors, leading to toxic consequences. We therefore investigated the efficiency of cross-seeding, by which aggregates of one polyQ sequence can act as seeds for elongation of the other sequence. We found that aggregates of both $K_2Q_{30}K_2$ (filled triangles) and $K_2Q_{15}HQHQ_{15}K_2$ (filled squares) are very good seeds for elongation of their self-peptides (Fig. 4C). We also found that $K_2Q_{15}HQHQ_{15}K_2$ (open diamonds) is essentially identical in its seeding ability for monomeric $K_2Q_{30}K_2$ as are $K_2Q_{30}K_2$ fibrils (filled triangles). Since the seed populations used for these experiments were matched in their concentrations of growing ends (Table I), these results can be taken directly as an indication of essentially equivalent molar seeding efficiencies of these two aggregates. This suggests that the ability of His insertion to suppress expanded polyQ toxicity does not lie in a reduced recruitment activity of the resulting amyloid aggregates.

Discussion

Different expanded CAG repeat diseases exhibit varying repeat length disease thresholds (Bates and Benn, 2002). Our group is exploring one possible explanation for these differences—that unique sequence features local to the polyQ in the disease proteins might modulate the aggressiveness of aggregation. For example, we found that the Pro-rich sequence on the C-terminal side of the polyQ segment in htt exon1 slows down aggregation and reduces aggregate stability, while not altering the fundamental aggregation mechanism (Bhattacharyya *et al*., 2006). In contrast, the N-terminal 17 amino acid long peptide of htt exon1 tremendously increases aggregation rate, due primarily to a dramatic change in aggregation mechanism (Thakur *et al*., 2009). Other polyQ disease proteins differ in their sizes and predicted structures, their intracellular locations and concentrations, the locations within the protein of their polyQ sequences, and their polyQ flanking sequences. Unique to these disease proteins is the sequence of AT-1, in which His residues are often found embedded within the polyQ sequences of benign proteins, but are absent from the expanded polyQ sequences found in disease-associated AT-1 proteins (Zoghbi and Orr, 1995). In one family, however, unaffected individuals contain His residues in polyQ stretches well above the pathological cutoff (Quan *et al*., 1995). We and others (Sen *et al*., 2003) are interested in the mechanism implied by this finding, in which His residues suppress polyQ toxicity.

Histidine and its imidazole side chain have a nitrogen atom with a pK_a of around 6.4 in a small molecule (Matthew, 1985) and a range of 5.5–8.1, with an average of 6.58, in two folded proteins (Matthew, 1985). There are several reports of aggregation kinetics being affected by histidine. Mulkerrin and Wetzel reported that in human IFN-γ, the side chains of non-protonated His residues can stimulate aggregation of the unfolded protein, and this can be suppressed by protonation, chemical modification or replacement of His residues (Mulkerrin and Wetzel, 1989). Similarly, Abedini and Raleigh showed that an islet amyloid polypeptide molecule, in which the only titratable group is a His residue, aggregates sluggishly at low pH and rapidly at high pH (Abedini and Raleigh, 2005). One mechanism by which unprotonated His residues are capable of mediating aggregation is by their ability to coordinate with bivalent metals like Zn^{+2}, as shown for fragments of the Alzheimer's plaque peptide Aβ (Morgan *et al*., 2002) and the human prion protein (Jobling *et al*., 2001). Owing to its aromatic ring structure, non-protonated histidine might contribute not only to generalized hydrophobic interactions, but also to more specific aromatic interactions, such as π–electron cloud effects (Burley and Petsko, 1986).

Consistent with the preliminary kinetic studies of Sen *et al*. (Sen *et al*., 2003), we show here that a His-Gln-His segment inserted into the middle of a polyQ tract significantly reduces—but does not eliminate—aggregation rates (Fig. 1). Interestingly, the degree by which $K_2Q_{15}HQHQ_{15}K_2$ aggregation is suppressed when compared with $K_2Q_{30}K_2$ is approximately the same at all pH values tested: 6.0, 7.5 and 8.5. Although the pK_a values of the His residues in monomeric $K_2Q_{15}HQHQ_{15}K_2$ are not known, it is almost certain

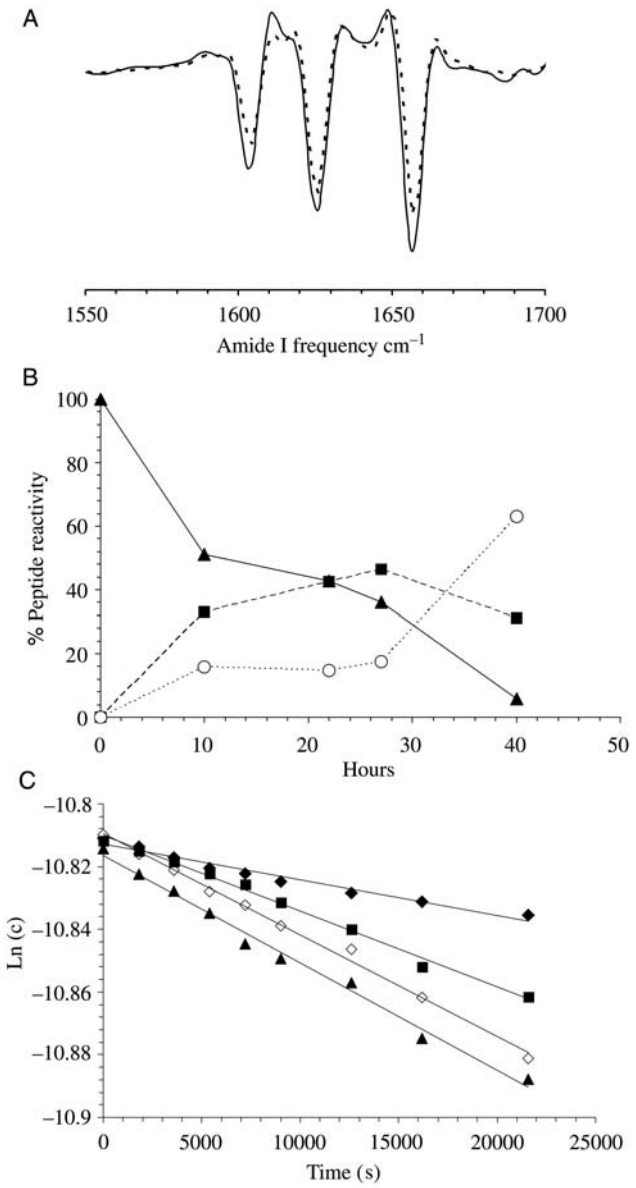

Fig. 4. Structures and properties of aggregates. (**A**) Second derivative FTIR spectra of fibrils, $K_2Q_{15}HQHQ_{15}K_2$ (continuous line) and $K_2Q_{30}K_2$ (broken line). (**B**) Reaction of His residues in $K_2Q_{15}HQHQ_{15}K_2$ fibrils with iodoacetate, determined by quantifying peptides by LC-MS from dissolved fibrils at various time points: unmodified peptide (filled triangles); singly-modified peptide (filled squares); doubly-modified peptide (open circles). (**C**) Cross-seeding efficiencies between polyQ peptides in PBSA at 37°C. Aggregate suspensions described in Fig. 3C were used to $K_2Q_{30}K_2$ and $K_2Q_{15}HQHQ_{15}K_2$ monomers at 5% (w/w). Elongation of monomeric $K_2Q_{30}K_2$ seeded with $K_2Q_{30}K_2$ aggregates (filled triangles, $R^2 = 0.991$) or $K_2Q_{15}HQHQ_{15}K_2$ aggregates (open diamonds, $R^2 = 0.9949$). Elongation of $K_2Q_{15}HQHQ_{15}K_2$ monomers seeded with $K_2Q_{15}HQHQ_{15}K_2$ aggregates (filled squares, $R^2 = 0.9934$) or $K_2Q_{30}K_2$ aggregates (filled diamonds, $R^2 = 0.9681$).

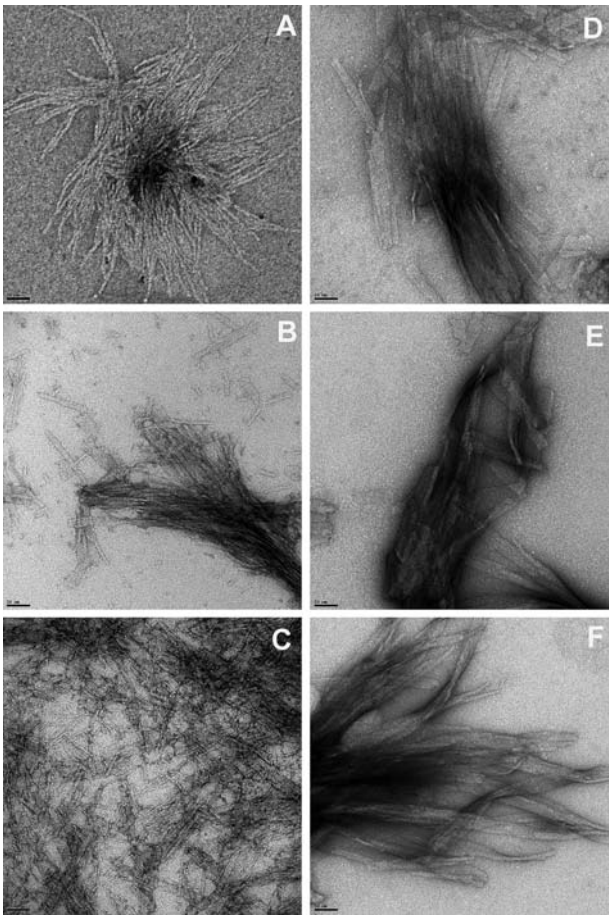

Fig. 5. Electron micrographs of fibrils harvested at the times indicated from reactions of polyQ peptides $K_2Q_{15}HQHQ_{15}K_2$ [pH 6.0, 648 h (**A**); pH 7.5, 412 h (**B**); pH 8.5, 364 h (**C**)] and $K_2Q_{30}K_2$ [pH 6.0, 512 h (**D**); pH 7.5, 240 h (**E**); pH 8.5, 162 h (**F**)]. Images were collected on a Technai 12 electron microscope on samples adsorbed onto freshly glow-charged carbon grids and stained with 1% uranyl acetate solution. Scale bar=50 nm.

that they are both essentially fully deprotonated at pH 8.5, where this peptide continues to aggregate more slowly than $K_2Q_{30}K_2$. It was not possible to meaningfully carry the pH series any lower than 6.0, because we found that aggregation of even the $K_2Q_{30}K_2$ peptide is nil at pH 5.5 (data not shown).

Detailed analysis of nucleation kinetics reveals that the major impact of inserted His residues in the pH 7.5–8.5 range is on the nucleation equilibrium constant, K_{n^*}. This value at pH 7.5 is diminished by 20.6-fold (Table I), corresponding to a $\Delta\Delta G_{n^*}$ of 1.86 kcal/mol. In contrast, the second-order elongation rate constant k_+, which also significantly contributes to overall nucleation efficiency (Slepko *et al*., 2006), is reduced at pH 7.5 only by 30% with the insertion of the His-Gln-His sequence into $K_2Q_{30}K_2$ (Table I). The modest effect on the elongation rate constant suggests that the presence of the His residues does not greatly impair the $K_2Q_{15}HQHQ_{15}K_2$ peptide's ability to undergo the 'dock and lock' (Esler *et al*., 2000; Nguyen *et al*., 2007) elongation cycle compared with unbroken polyQ.

His protonation is very likely to play a role in the aggregation of $K_2Q_{15}HQHQ_{15}K_2$ as the pH is shifted from 7.5 to 6.0, where there appears to be a fundamental change in the mechanism of aggregation. At pH 6.0, compared with pH 7.5, there is a dramatic discontinuity between the ThT determination of reaction progress and the sedimentation assay assessment (Fig. 1C). This is qualitatively similar to the aggregation of htt exon1 peptides, in which formation of a ThT-negative, spherical oligomeric intermediate by downhill aggregation precedes the nucleation of an amyloid center (Thakur *et al*., 2009). In fact, the EM morphology of the pH 6.0 aggregates of $K_2Q_{15}HQHQ_{15}K_2$ (Fig. 5A) is remarkably

similar to that for htt exon1 aggregates grown at pH 7.5 (Thakur *et al*., 2009). The ThT response per mass of aggregate is also much higher for pH 6.0 $K_2Q_{15}HQHQ_{15}K_2$ aggregates than for pH 7.5 aggregates (Fig. 1B), likewise consistent with a different morphology. The main difference between the pH 6.0 versus pH 7.5 aggregation of $K_2Q_{15}HQHQ_{15}K_2$ and the effect of htt exon1 sequence context on simple polyQ aggregation (Thakur *et al*., 2009) is that, in the latter, the new mechanism occurs at a dramatically accelerated rate, while, in the former, the new mechanism occurs at a much slower rate. This suggests that, whatever the details of the pH 6.0 mechanism for $K_2Q_{15}HQHQ_{15}K_2$ aggregation, one contributing factor must be the ability of His protonation to suppress the normal, neutral pH mechanism.

Can these kinetic effects of histidine insertion tell us anything about the nature of the critical nucleus? All we know about the nucleus is that it is a rare monomeric state. The ground state for polyQ monomers in water is a collapsed coil (Crick *et al*., 2006) that is not, however, as compact as a folded, globular protein (Thakur *et al*., 2009). There are two possible kinds of states one can imagine that might be (a) of higher energy than a collapsed coil and (b) empowered to initiate amyloid formation. In Model A, elements of the polyQ chain might transiently snake out of the collapsed coil to achieve a more extended, solvated chain that would be available for forming intermolecular H-bonds with other molecules. In Model B, the collapsed polyQ could transiently organize internally, through formation of intramolecular H-bonds, into more defined structures with β-sheet content capable of undergoing an initial elongation step that would be very similar to the fibril elongation steps later.

As described above, at pH values where His in the monomer is unlikely to be protonated, His insertion significantly destabilizes the nucleus. His and Gln have roughly the same side chain volumes and H-bonding capabilities, and non-protonated His is also similar to Gln in free energies of transfer from organic solvents to water (Radzicka *et al*., 1988) and in virtual free energies in distribution from the interior to the exterior of folded proteins (Chothia, 1976). According to this analysis, the hypothetical "collapsed to extended" transition in Model A for the nucleus would be expected to be relatively unaffected by His insertion into polyQ. It is difficult to predict the effect of His insertion on the stability of a folded nucleus, as in Model B, without knowing the details of this organized structure.

As described above, at pH 6.0 where His in the monomer is likely to be at least partially protonated, the aggregation reaction (a) slows down and (b) occurs by a different mechanism. This suggests that either the nucleation equilibrium or the elongation rate constant for the normal, neutral pH mechanism must be significantly diminished by His protonation. If the nucleus state is as described in Model A, one would expect protonation to actually favor nucleation, rather than suppress it; we have no data to address the possible effect of pH 6.0 on $K_2Q_{15}HQHQ_{15}K_2$ aggregate elongation. It is again difficult to predict the effect of protonation on formation of the Model B nucleus, although intuitively this might be expected to be minor if the folded nucleus resembles the folded fibril with its solvent-exposed His residues.

While no firm conclusions can be drawn from our data about the nature of the kinetic nucleus for polyQ aggregation, we believe that the above analysis suggests the feasibility of using classical protein structure–function approaches, coupled with nucleation kinetics analysis, to address this question.

It is also possible to estimate the thermodynamic impact of the His-Gln-His insertion on the equilibrium position of the aggregation reaction, a parameter that, like K_{n^*}, is a measure of the ΔG between the monomer ensemble and another state. The C_r for $K_2Q_{15}HQHQ_{15}K_2$ aggregation at pH 7.5 is 0.63 ± 0.07 μM (Fig. 1C), corresponding to a ΔG for the aggregation reaction of -8.79 kcal/mol. In contrast, the C_r for $K_2Q_{30}K_2$ aggregation at pH 7.5, estimated from the last time points of the forward aggregation reaction (Fig. 1A), is 0.21 μM. This corresponds to a $\Delta\Delta G_{agg}$ between the $K_2Q_{30}K_2$ and $K_2Q_{15}HQHQ_{15}K_2$ aggregation reactions of -0.71 kcal/mol. (It is possible, even likely, that the C_r for $K_2Q_{30}K_2$ is lower than 0.2 μM.) Thus, the impact of the His-Gln-His insertion into polyQ is somewhat greater on the nucleation equilibrium at pH 7.5 (approximately 21-fold) than on the final aggregate assembly equilibrium (approximately 3-fold). While nucleation thermodynamics is determined by the folding of the solvated monomer into a solvated nucleus, elongation thermodynamics is determined by the folding of the monomer onto a fibril template, where some stabilization energy is expected to be gained from intermolecular contacts that are not available in nucleus formation. It seems reasonable, then, that the impact of a mutation might be greater at the monomeric nucleation stage, even if the folding of the peptide is similar in the nucleus and as a subunit of a fibril. Of course, the structure of polyQ in either state is not known in any detail, although the rough organization within the fibril is well-documented (Sharma *et al*., 2005).

Here, we show that the His residues are surface-exposed and accessible to alkylation (Fig. 4B) in the final aggregate structure. This is entirely consistent with the hypothesis that the His residues are placed in reversed turns and excluded from the packed β-sheets in the assembled amyloid fibril (Sen *et al*., 2003); however, the possibility that His residues are in β-sheet, but with side chains projecting into solvent, cannot be formally excluded by our data. While much remains to be learned about the role of aggregation in expanded polyQ repeat diseases, it is interesting that the results presented here are yet another example of a subtle change in a polyQ protein or its environment that affects aspects of both aggregation and toxicity. Besides the exhaustively reported data on the toxic and aggregation effects of repeat length increases themselves, other examples include the ability of the Pro-rich domain of htt exon1 to suppress both intracellular aggregate formation and toxicity in a yeast model (Duennwald *et al*., 2006), and the ability of co-expressed short polyQ peptides to enhance both aggregation and toxicity in a *Drosophila* model (Slepko *et al*., 2006).

Individuals with expanded polyQ sequences in AT-1 that are, however, interrupted with His residues do not develop SCA1 (Quan *et al*., 1995). This suggests that the His interruptions somehow compromise the normal toxicity associated with expanded polyQ. It is possible that this effect has something to do with protein aggregation. We describe here the results of a number of comparisons of unbroken polyQ with polyQ containing a central HQH motif. At neutral pH,

inserted His residues suppress aggregation by decreasing the thermodynamic stability of the kinetic nucleus. Inserted His residues also somewhat decrease the stability of aggregates in the elongation equilibrium. There does not appear to be a huge effect on structure, and the ability of aggregates of His-containing polyQ to seed elongation by unbroken polyQ, as required for a recruitment mechanism of toxicity, is not significantly altered. At pH 6.0, not only does His insertion reduce aggregation rate, it also appears to change the aggregation mechanism and alter the final aggregate structure. This mechanism and rate change by a modest pH shift might play a role *in vivo*, if AT-1 in its cellular life were to experience a pH 6.0 environment. Taken together, the ability of inserted His residues to reduce aggregation kinetics at pH values relevant to cell biology is consistent with SCA1 genetics which suggest that His insertions in expanded polyQ sequences in the AT-1 protein block toxicity.

Acknowledgements

We thank Ashwani Thakur and Anusri Bhattacharyya for help with the nucleation kinetics analysis.

Funding

This work was supported by the National Institutes of Health (R01 AG019322 to R.W.) and by a research contract from the Hereditary Disease Foundation (to R.W.).

References

Abedini,A. and Raleigh,D.P. (2005) *Biochemistry*, **44**, 16284–16291.
Apostol,B.L., *et al*. (2003) *Proc. Natl Acad. Sci. USA*, **100**, 5950–5955.
Bates,G.P. and Benn,C. (2002) In Bates,G.P., Harper,P.S. and Jones,L. (eds.), *Huntington's Disease*. Oxford University Press, Oxford, UK, pp. 429–472.
Bauer,P.O., Matoska,V., Zumrova,A., Boday,A., Doi,H., Marikova,T. and Goetz,P. (2005) *J. Appl. Genet.*, **46**, 325–328.
Bhattacharyya,A.M., Thakur,A.K. and Wetzel,R. (2005) *Proc. Natl Acad. Sci. USA*, **102**, 15400–15405.
Bhattacharyya,A., Thakur,A.K., Chellgren,V.M., Thiagarajan,G., Williams,A.D., Chellgren,B.W., Creamer,T.P. and Wetzel,R. (2006) *J. Mol. Biol.*, **355**, 524–535.
Burley,S.K. and Petsko,G.A. (1986) *FEBS Lett.*, **203**, 139–143.
Chen,S., Berthelier,V., Yang,W. and Wetzel,R. (2001) *J. Mol. Biol.*, **311**, 173–182.
Chen,S., Berthelier,V., Hamilton,J.B., O'Nuallain,B. and Wetzel,R. (2002a) *Biochemistry*, **41**, 7391–7399.
Chen,S., Ferrone,F. and Wetzel,R. (2002b) *Proc. Natl Acad. Sci. USA*, **99**, 11884–11889.
Chothia,C. (1976) *J. Mol. Biol.*, **105**, 1–12.
Chung,M.Y., Ranum,L.P., Duvick,L.A., Servadio,A., Zoghbi,H.Y. and Orr,H.T. (1993) *Nat. Genet.*, **5**, 254–258.
Collins,S.R., Douglass,A., Vale,R.D. and Weissman,J.S. (2004) *PLoS Biol.*, **2**, e321.
Crestfield,A.M., Stein,W.H. and Moore,S. (1963) *J. Biol. Chem.*, **238**, 2421–2428.
Crick,S.L., Jayaraman,M., Frieden,C., Wetzel,R. and Pappu,R.V. (2006) *Proc. Natl Acad. Sci. USA*, **103**, 16764–16769.
Duennwald,M.L., Jagadish,S., Muchowski,P.J. and Lindquist,S. (2006) *Proc. Natl Acad. Sci. USA*, **103**, 11045–11050.
Esler,W.P., Stimson,E.R., Jennings,J.M., Vinters,H.V., Ghilardi,J.R., Lee,J.P., Mantyh,P.W. and Maggio,J.E. (2000) *Biochemistry*, **39**, 6288–6295.
Ferrone,F. (1999) *Methods Enzymol.*, **309**, 256–274.
Fraser,P.E., McLachlan,D.R., Surewicz,W.K., Mizzen,C.A., Snow,A.D., Nguyen,J.T. and Kirschner,D.A. (1994) *J. Mol. Biol.*, **244**, 64–73.
Frontali,M., Novelletto,A., Annesi,G. and Jodice,C. (1999) *Phil. Trans. R. Soc. Lond. B Biol. Sci.*, **354**, 1089–1094.
Huang,C.C., Faber,P.W., Persichetti,F., Mittal,V., Vonsattel,J.P., MacDonald,M.E. and Gusella,J.F. (1998) *Somat. Cell Mol. Genet.*, **24**, 217–233.
Jackson,M. and Mantsch,H.H. (1995) *Crit. Rev. Biochem. Mol. Biol.*, **30**, 95–120.
Jobling,M.F., *et al*. (2001) *Biochemistry*, **40**, 8073–8084.
Klein,F.A., Pastore,A., Masino,L., Zeder-Lutz,G., Nierengarten,H., Oulad-Abdelghani,M., Altschuh,D., Mandel,J.L. and Trottier,Y. (2007) *J. Mol. Biol.*, **371**, 235–244.
Klement,I.A., Skinner,P.J., Kaytor,M.D., Yi,H., Hersch,S.M., Clark,H.B., Zoghbi,H.Y. and Orr,H.T. (1998) *Cell*, **95**, 41–53.
Krobitsch,S. and Lindquist,S. (2000) *Proc. Natl Acad. Sci. USA*, **97**, 1589–1594.
Matsuyama,Z., Izumi,Y., Kameyama,M., Kawakami,H. and Nakamura,S. (1999) *J. Med. Genet.*, **36**, 546–548.
Matthew,J.B. (1985) *Annu. Rev. Biophys. Biophys. Chem.*, **14**, 387–417.
McCampbell,A., *et al*. (2000) *Hum. Mol. Genet.*, **9**, 2197–2202.
Morgan,D.M., Dong,J., Jacob,J., Lu,K., Apkarian,R.P., Thiyagarajan,P. and Lynn,D.G. (2002) *J. Am. Chem. Soc.*, **124**, 12644–12645.
Morley,J.F., Brignull,H.R., Weyers,J.J. and Morimoto,R.I. (2002) *Proc. Natl Acad. Sci. USA*, **99**, 10417–10422.
Mulkerrin,M.G. and Wetzel,R. (1989) *Biochemistry*, **28**, 6556–6561.
Nguyen,P.H., Li,M.S., Stock,G., Straub,J.E. and Thirumalai,D. (2007) *Proc. Natl Acad. Sci. USA*, **104**, 111–116.
Nucifora,F.C., Jr, *et al*. (2001) *Science*, **291**, 2423–2428.
O'Nuallain,B., Shivaprasad,S., Kheterpal,I. and Wetzel,R. (2005) *Biochemistry*, **44**, 12709–12718.
O'Nuallain,B., Thakur,A.K., Williams,A.D., Bhattacharyya,A.M., Chen,S., Thiagarajan,G. and Wetzel,R. (2006) *Methods Enzymol.*, **413**, 34–74.
Orr,H.T., Chung,M.Y., Banfi,S., Kwiatkowski,T.J., Jr, Servadio,A., Beaudet,A.L., McCall,A.E., Duvick,L.A., Ranum,L.P. and Zoghbi,H.Y. (1993) *Nat. Genet.*, **4**, 221–226.
Osmand,A.P., Berthelier,V. and Wetzel,R. (2006) *Methods Enzymol.*, **412**, 106–122.
Perez,M.K., Paulson,H.L., Pendse,S.J., Saionz,S.J., Bonini,N.M. and Pittman,R.N. (1998) *J. Cell. Biol.*, **143**, 1457–1470.
Preisinger,E., Jordan,B.M., Kazantsev,A. and Housman,D. (1999) *Phil. Trans. R. Soc. Lond. B Biol. Sci.*, **354**, 1029–1034.
Quan,F., Janas,J. and Popovich,B.W. (1995) *Hum. Mol. Genet.*, **4**, 2411–2413.
Radzicka,A., Pedersen,L. and Wolfenden,R. (1988) *Biochemistry*, **27**, 4538–4541.
Scherzinger,E., Lurz,R., Turmaine,M., Mangiarini,L., Hollenbach,B., Hasenbank,R., Bates,G.P., Davies,S.W., Lehrach,H. and Wanker,E.E. (1997) *Cell*, **90**, 549–558.
Sen,S., Dash,D., Pasha,S. and Brahmachari,S.K. (2003) *Protein Sci.*, **12**, 953–962.
Sharma,D., Sharma,S., Pasha,S. and Brahmachari,S.K. (1999) *FEBS Lett.*, **456**, 181–185.
Sharma,D., Shinchuk,L.M., Inouye,H., Wetzel,R. and Kirschner,D.A. (2005) *Proteins*, **61**, 398–411.
Shivaprasad,S. and Wetzel,R. (2006) *J. Biol. Chem.*, **281**, 993–1000.
Slepko,N., Bhattacharyya,A.M., Jackson,G.R., Steffan,J.S., Marsh,J.L., Thompson,L.M. and Wetzel,R. (2006) *Proc. Natl Acad. Sci. USA*, **103**, 14367–14372.
Thakur,A. and Wetzel,R. (2002) *Proc. Natl Acad. Sci. USA*, **99**, 17014–17019.
Thakur,A.K., *et al*. (2009) *Nat. Struct. Mol. Biol.*, **16**, 380–389.
Wetzel,R. (2009) In Dobson,C.M., Kelly,J.W. and Ramirez-Alvarado,M. (eds.), *Protein Misfolding Diseases: Current and Emerging Principles and Therapies*. Wiley, New York, in press.
Zoghbi,H.Y. and Orr,H.T. (1995) *Semin. Cell. Biol.*, **6**, 29–35.

Received May 18, 2009; revised May 18, 2009; accepted May 19, 2009

Edited by Steve Bottomley